Photochemistry and Photobiology, 2010, 86: 23–30

A Comparative Kinetic and Mechanistic Study Between Tetrahydrozoline and Naphazoline Toward Photogenerated Reactive Oxygen Species

Susana Criado* and Norman A. García

Departamento de Química, Universidad Nacional de Río Cuarto, Campus Universitario, Río Cuarto, Argentina

Received 23 February 2009, accepted 5 July 2009, DOI: 10.1111/j.1751-1097.2009.00616.x

ABSTRACT

Kinetic and mechanistic aspects of the vitamin B2 (riboflavin [Rf])-sensitized photo-oxidation of the imidazoline derivates (IDs) naphazoline (NPZ) and tetrahydrozoline (THZ) were investigated in aqueous solution. The process appears as important on biomedical grounds, considering that the vitamin is endogenously present in humans, and IDs are active components of ocular medicaments of topical application. Under aerobic visible light irradiation, a complex picture of competitive interactions between sensitizer, substrates and dissolved oxygen takes place: the singlet and triplet (^{3}Rf*) excited states of Rf are quenched by the IDs: with IDs concentrations *ca.* 5.0 mM and 0.02 mM Rf, ^{3}Rf* is quenched by IDs, in a competitive fashion with dissolved ground state oxygen. Additionally, the reactive oxygen species: $O_2(^1\Delta_g)$, $O_2^{\bullet-}$, $HO^\bullet$ and H_2O_2, generated from ^{3}Rf* and $Rf^{\bullet-}$, were detected with the employment of time-resolved methods or specific scavengers. Oxygen uptake experiments indicate that, for NPZ, only H_2O_2 was involved in the photo-oxidation. In the case of THZ, $O_2^{\bullet-}$, $HO^\bullet$ and H_2O_2 were detected, whereas only $HO^\bullet$ was unambiguously identified as THZ oxidative agents. Upon direct UV light irradiation NPZ and THZ generate $O_2(^1\Delta_g)$, with quantum yields of 0.2 (literature value, employed as a reference) and 0.08, respectively, in acetonitrile.

INTRODUCTION

The photochemical degradation of medicinal drugs is being increasingly investigated in the last decades, especially under daylight irradiation (1,2). Problems related to drug photostability are of relevance not only in the context of UV–visible exposure after topical application on skin or eyes, but also in their production and storage (3).

Although photoreactions on medicinal drugs could give rise to products with different, null or even undesirable bioactivity, most common drugs with pharmaceutical relevance are transparent to daylight. However, photodamage could occur through the photodynamic action of other compounds usually coadministered, or tissular molecules belonging to the biological environment able to absorb environmental light (1,4,5).

Riboflavin (Rf), one of the components of the B2-vitamin complex, has been postulated as a viable sensitizer for the *in vivo* photo-oxidative degradation of relevant natural or externally added substrates in different organisms (6). In this way, a new method of collagen cross-linking by the sensitizer Rf and UVA light has been developed for the treatment of progressive keratoconus (7–9). Other possible clinical applications of corneal collagen cross-linking lie in the field of refractive surgery, corneal ulcers, stromal melting and thinning (8,9). It is known that Rf can act *via* the generation of singlet molecular oxygen, $O_2(^1\Delta_g)$ (type II mechanism) and/or *via* radical species (type I mechanism), including reactive oxygen species (ROS) such as superoxide radical anion ($O_2^{\bullet-}$), hydroxyl radical ($HO^\bullet$) and hydrogen peroxide (H_2O_2) (10). Moreover, Rf can also directly oxidize a suitable substrate by electron abstraction in the absence of molecular oxygen (11).

Other pigments with sensitizing properties are the collectively known "age pigments." Although these pigments are a highly heterogeneous mixture, two types can be distinguished: advanced glycation end-products and lipofuscin. Both have been identified as natural ocular photosensitizers (12). Research suggests that aerobic irradiation of N-retinylidene-N-retinylethanol-amine, one of the constituents that has been characterized, or whole lipofuscin, with short-wavelength visible light, brings about the generation of ROS including $O_2(^1\Delta_g)$, $O_2^{\bullet-}$ and perhaps $HO^\bullet$ (13–15).

In the context, the presence of Rf, lipofuscin or any suitable molecule that can act as photosensitizer by absorbing visible light could start an unpredictable series of photoreactions, many of them driven through the action of the ROS.

For this study, we have selected two imidazoline ocular decongestants (generically named IDs in what follows) naphazoline (NPZ) and tetrahydrozoline (THZ); their structural formulae are shown in Scheme 1. Their primary mechanism of action is vasoconstriction, accomplished by direct stimulation of alpha receptors on blood vessels (16–20). NPZ is a drug available in the market as a component of eye drops. It is widely used to relieve redness because of minor eye irritation, caused by cold, dust, wind, smog, pollen, swimming or wearing contact lenses (21). THZ is available as an over-the-counter medication for treatment of eye irritation and nasal congestion (16). As vitamin Rf and IDs can occupy common locations in complex biological structures, kinetic information about visible light photopromoted interactions between these compounds can help understand the behavior of Rf-generated oxidative species in general, the potential *in vivo* or *in vitro* photoreactions on IDs in particular, and the

*Corresponding author email: scriado@exa.unrc.edu.ar (Susana Criado)

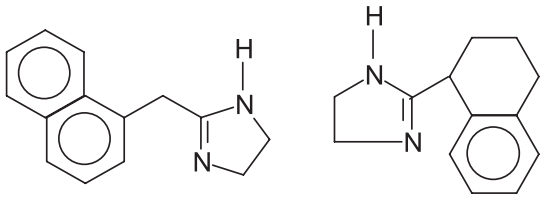

Naphazoline (NPZ) Tetrahydrozoline (THZ)

Scheme 1. Chemical structures of naphazoline and tetrahydrozoline.

propensity of such processes to occur under given environmental conditions. Besides, this knowledge could help in the design of more photostable drugs as well as in the development of photoprotective mechanisms against adverse potential phototoxic reactions triggered by drugs or by other substrates naturally present in the biological environment.

The purpose of the present work was to analyze the behavior of Rf as a sensitizer for the photodecomposition of NPZ and THZ, to get information about the behavior of the visible light photopromoted interactions taking place between these drugs and biologically relevant oxidative entities, generated under photosensitizing conditions.

MATERIALS AND METHODS

Chemicals. Naphazoline (2-(naphthalen-4-ylmethyl-4,5-dihydro-1H-imidazole), tetrahydrozoline (2-tetralin-1-yl-4,5-dihydro-1H-imidazole), Rf, perinaphthenone (PN), sodium azide (NaN_3), D-mannitol, catalase from bovine liver (CAT) and superoxide dismutase (SOD) from bovine erythrocytes were purchased from Sigma Chem. Co. Furfuryl alcohol was purchased from Riedel de Haën. Benzoic acid sodium salt was provided by Aldrich and H_2O_2 by Tensol. The solvents employed were methanol (MeOH) and acetonitrile (MeCN) HPLC quality, from Sintorgan; D_2O, 99.9% from Aldrich and triply distilled H_2O from Chemical Department Laboratories-UNRC.

Stationary photolysis. O_2 ($^1\Delta_g$) was generated by irradiation of the solutions containing the sensitizer plus the individual IDs, at wavelengths greater than 300 nm. Cut-off filters ensured that the light was absorbed only by the sensitizer. Light from a 150 W quartz–halogen lamp was passed through a water filter and focused on the reaction vessel (either a hermetically sealed reaction cell with an oxygen electrode, or a 1 × 1 cm spectrophotometric cuvette) containing the continuously stirred aerated solutions.

The experiments of oxygen uptake by IDs solutions (*ca*. 5.0 mM) in water were determined with the specific oxygen electrode Orion 97-08.

The Rf-photosensitized rates of oxygen consumption were determined by evaluation of the initial slopes of oxygen uptake *vs*. irradiation time. To investigate the eventual involvement of ROS, experiments of oxygen uptake in the absence and in the presence of different additives with ROS-scavenging capacity were made. The following compounds were employed as ROS scavengers: 5.0 mM NaN_3 for $O_2(^1\Delta_g)$, 1 mg per 100 mL SOD for $O_2^{\bullet-}$, 1 mg per 100 mL CAT for H_2O_2 and 5.0 mM D-mannitol and 5.0 mM benzoic acid sodium salt for $HO^{\bullet}$.

The anaerobic (N_2 bubbling) photodegradation rates of 0.02 mM Rf in the presence and in the absence of *ca*. 0.1 mM IDs were deduced from the absorption spectrum by evaluating the absorbance decay at 445 nm, a region where only Rf absorbs.

Stationary and time-resolved fluorescence. For the stationary fluorescence experiments, a Spex Fluoromax spectrofluorometer was employed, at 25 ± 1°C in air-equilibrated solutions. Fluorescence lifetimes were measured using a time-correlated single photon counting technique (SPC) on an Edinburgh FL-9000CD instrument.

In the Rf fluorescence experiments MeOH was used, instead of water, as solvent to enhance the solubility of IDs. The excitation and emission wavelengths were 445 and 515 nm, respectively. To determine the values of ^1k_q, a classical Stern–Volmer treatment of the data was applied through Eq. (1), where $^1\tau$ and $^1\tau_0$ are the respective fluorescence lifetimes of Rf in the presence and in the absence of IDs.

$$^1\tau_0/^1\tau = 1 + {}^1k_q{}^1\tau_0\ [\mathrm{IDs}] \quad (1)$$

The direct reaction between 2.0 mM NPZ and 20.0 mM H_2O_2 was evaluated through the respective fluorescence spectra (λ_{exc} = 315 nm and λ_{em} = 333 nm) of the imdazoline in aqueous solution, after and before addition of the peroxide.

Ground state absorption spectra were registered in a Hewlett-Packard 8452A diode array spectrophotometer. In all cases, quartz cells of 1.0 cm path-length were employed.

Laser flash photolysis experiments. N_2-saturated methanolic solutions of 0.01 mM Rf were photolysed using a flash photolysis apparatus with the frequency-doubled output of a Nd:YAG laser system (Spectron) at 355 nm as excitation source, employing a 150 W xenon lamp as analyzing light. The detection system comprised a photon technology international monochromator and a red-extended photomultiplier (Hamamatsu R666). The signal, acquired and averaged by a digital oscilloscope (Hewlett-Packard 54504A), was transferred to a PC *via* a Hewlett-Packard interface bus parallel interface, where it was analyzed and stored.

The disappearance of ^{3}Rf*, generated by the 355 nm laser pulse, was monitored from the first-order decay of the absorbance at 670 nm, a zone where the interference from other possible species is negligible. ^{3}Rf* decay was measured at low Rf concentration (typically 0.02 mM) and at low enough laser energy, to avoid undesirable effects such as self-quenching and triplet–triplet annihilation, respectively. A Stern–Volmer treatment was applied (Eq. 2) to determine the values of $3k_q$.

$$^3\tau_0/^3\tau = 1 + {}^3k_q{}^3\tau_0\ [\mathrm{IDs}], \quad (2)$$

where $^3\tau$ and $^3\tau_0$ are the respective lifetimes of ^{3}Rf* in the presence and in the absence of IDs.

The transient absorption spectra of 0.02 mM Rf and 0.02 mM Rf + 5.0 mM IDs were determined in N_2-saturated methanolic solutions, using a flash photolysis apparatus, described above. MeOH was employed as a solvent in laser flash photolysis experiments to enhance the IDs solubility.

Time-resolved O_2 ($^1\Delta_g$) phosphorescence detection. The laser-kinetic spectrophotometer for time-resolved O_2 ($^1\Delta_g$) phosphorescence detection (TRPD) has been previously described (22). Briefly, it consisted of a Nd:YAG laser (Spectron) as the excitation source. The output at 355 nm was employed to excite the sensitizer PN. The emitted radiation (mainly 1270 nm) was detected at right angles using an amplified Judson J16/8Sp germanium detector, after passing through appropriate filters. The output of the detector was coupled to a digital oscilloscope and to a personal computer for processing the signal. Sixteen shots were usually averaged to get a good signal-to-noise ratio, from which the decay times were calculated. Solutions with absorbance at the laser wavelength of 0.2 were employed. The decay kinetics was first order in all cases. The experiments were made in D_2O, because of the enlargement of the O_2 ($^1\Delta_g$) lifetime in this solvent (23). O_2 ($^1\Delta_g$) lifetimes were evaluated in the presence (τ) and in the absence (τ_0) of IDs. If the ratio τ_0/τ is plotted as a function of the quencher concentration, the overall rate constant for O_2 ($^1\Delta_g$) quenching, k_t (addition $k_q + k_r$, processes [10] and [11], respectively, in Scheme 2) could be determined.

Determination of the reactive rate constants k_r. The rate constant of the chemical reaction of 5.0 mM IDs with $O_2(^1\Delta_g)$, k_r (process [11] in Scheme 2), was determined using an actinometric method, already described in other papers, which is based on the comparison of the slopes of the time course (*pseudo* first-order plots) of oxygen uptake by the substrate (5.0 mM) and of a reference compound (5.0 mM) with known k_r value (k_{rR}) (24). The ratio of the *pseudo* first-order slopes of oxygen uptake by IDs and a reference ($slope_{IDs}/slope_R$), both determined at identical concentration, is equal to k_r/k_{rR}, assuming that the reaction of $O_2(^1\Delta_g)$ with the quencher is the only way for oxygen consumption.

Determination of O_2 ($^1\Delta_g$) quantum yields (Φ_Δ). The quantum yield of O_2 ($^1\Delta_g$) production by THZ, in MeCN, was determined employing NPZ as a reference. The initial intensities of the emission at 1270 nm were measured for optically matched solutions of THZ and NPZ. The 266 nm output of the already mentioned Spectron Nd:YAG laser was used as excitation source. We employed a Φ_Δ value for $O_2(^1\Delta_g)$ production by the reference of 0.2 in MeCN (21).

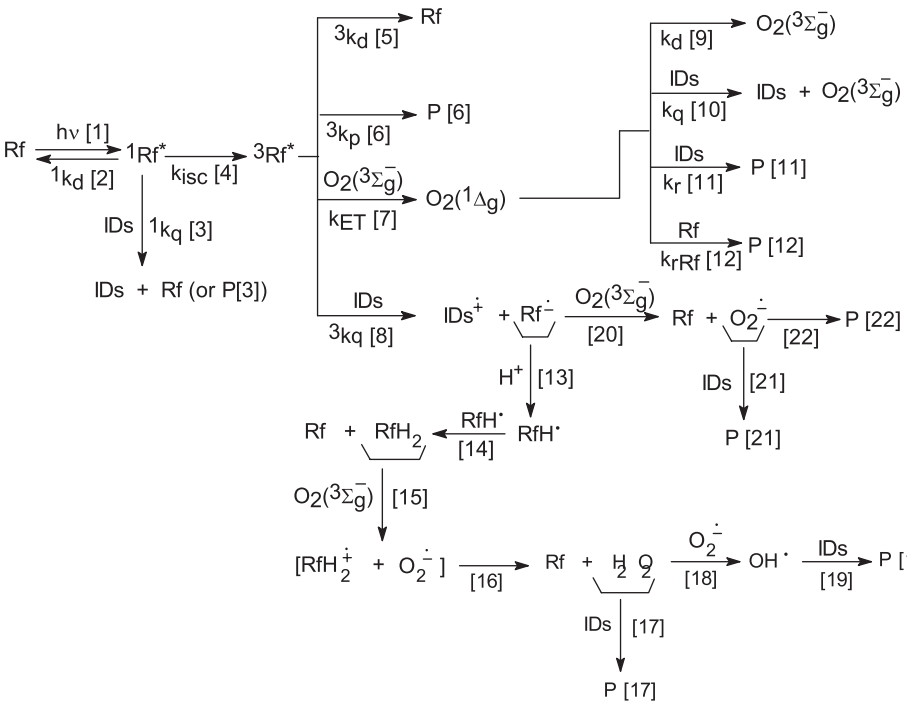

Scheme 2. Possible reaction pathways in the riboflavin-sensitized photoirradiation of naphazoline and tetrahydrozoline (IDs in the Scheme).

RESULTS

Sensitized photoirradiation of IDs

Photoirradiation at wavelength >300 nm, a spectral region where the IDs are transparent, of air-equilibrated aqueous solutions of 0.02 mM Rf and either 0.1 mM THZ or NPZ produced changes in the absorption spectra of the IDs (Fig. 1), thus indicating the occurrence of chemical transformations. No spectral changes were observed in the absence of light. Although in-dark associations between Rf and different *N*-heteraromatic compounds have been previously observed (23,25) no spectral perturbations because of this process could be detected in the differential absorption spectra of solutions containing Rf and IDs, within the concentration range employed in this work.

On the other hand, we observed that both the anaerobic and the aerobic photodegradation rates of Rf, processes that are well known to occur anaerobically from ^{3}Rf* and/or aerobically *via* O_2 ($^1\Delta_g$) (26,27), suffer a decrease in the presence of 0.1 mM IDs (Fig. 2). Besides, the comparison of the respective absorption spectra obtained under aerobic and anaerobic conditions of each ID upon Rf-sensitized photoirradiation are different from each other, indicating the appearance of different photoproducts (see Fig. 1 for an illustration in the case of NPZ).

Finally, oxygen consumption was observed in the photoirradiation of aqueous solutions of 5.0 mM IDs + 0.02 mM Rf (Fig. 1), but not in the dark or in the absence of IDs.

The above-mentioned preliminary pieces of experimental evidence clearly indicate the existence of interactions between IDs and ^{1}Rf* and/or ^{3}Rf*, and/or ROS generated upon photoexcitation of the pigment. To elucidate kinetic and mechanistic aspects of the mentioned interactions and to identify possible ROS involved in the degradation of the substrates a systematic study was developed, employing the set of reactions shown in Scheme 2 for interpretation and discussion of the results.

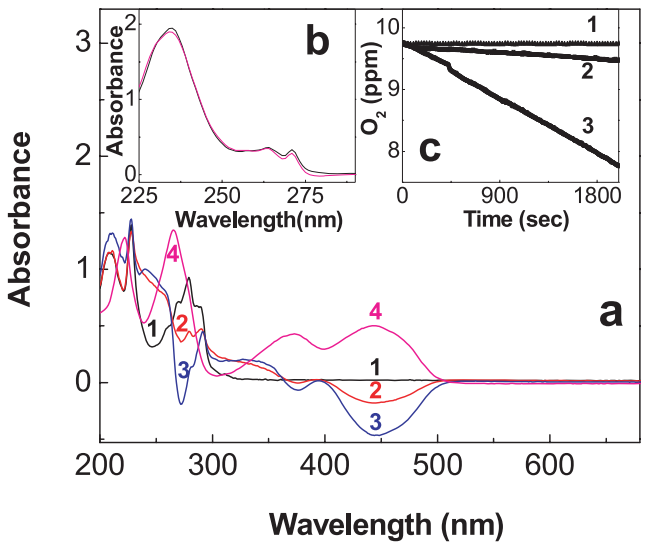

Figure 1. (a) Spectral evolution of 0.12 mM naphazoline + 0.02 mM riboflavin *vs.* 0.02 mM riboflavin upon visible light photoirradiation: 1, non-irradiated; 2, irradiated 290 min (aerated); 3, irradiated 180 min (in absence of oxygen); 4, absorption spectrum UV–visible of 0.02 mM riboflavin *vs.* water, included for comparative purposes. (b) Spectral evolution of 0.47 mM tetrahydrozoline + 0.02 mM riboflavin *vs.* 0.02 mM riboflavin upon visible light photoirradiation: upper curve, none irradiated; lower curve, irradiated 60 min (aerated). (c) Oxygen consumption upon photoirradiation: 1, 0.02 mM riboflavin + 1.0 mM naphazoline; 2, 0.02 mM riboflavin + 1.0 mM tetrahydrozoline; 3, 0.02 mM riboflavin. Solvent: H_2O.

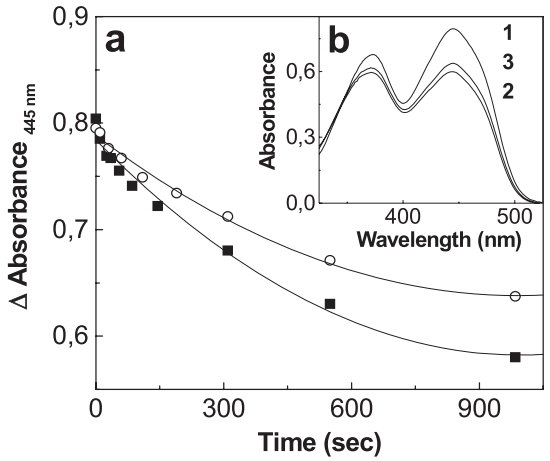

Figure 2. (a) Relative absorbance decreases at 445 nm of solutions of riboflavin as a function of the visible light irradiation time: (■) 0.02 mM riboflavin; (○) 0.02 mM riboflavin in presence of 1.0 mM naphazoline. (b) Spectral changes in a solution of 0.02 mM riboflavin upon visible light photoirradiation: 1, without additives, non-irradiated; 2, without additives 985 s irradiation; 3, 985 s irradiation, in the presence of 0.1 mM naphazoline. All the experiments were made in N_2-saturated solutions. Solvent: H_2O.

Scheme 2 depicts a generic photosensitized process, in which the absorption of incident light promotes the sensitizer (Rf, in ground state)) to ^{1}Rf* (process [1]) and/or ^{3}Rf* (process [4]) states. Both states can either decay or be quenched to ground state Rf through processes [2–8]. An energy transfer process from ^{3}Rf* to $O_2(^3\Sigma_g^-)$ dissolved in the medium, can yield the species $O_2(^1\Delta_g)$ (process [7]) that can decay either by collision with surrounding solvent molecules (process [9]) or by interaction with IDs through physical (step [10]) and/or chemical (step [11]) process. An electron transfer process from ^{3}Rf* to IDs would give rise to the respective semireduced ($Rf^{\bullet-}$) and semioxidized ($IDs^{\bullet+}$) forms (process [8]). The interaction of $Rf^{\bullet-}$ with $O_2(^3\Sigma_g^-)$ could generate the reactive species $O_2^{\bullet-}$ through process [19] (reported (28,29) $k_{19} = 1.4 \times 10^8$ M^{-1}s^{-1}). At pH 6, the neutral Rf radical ($RfH^{\bullet}$) ($pK_a = 8.3$) would be formed (30,31) after the protonation of the species $Rf^{\bullet-}$ (process [13]), generated through process [8]. The bimolecular decay of $RfH^{\bullet}$ is known (28,32) to proceed through disproportion reaction to yield equimolar Rf and fully reduced Rf (RfH_2) (process [14]), which in the presence of $O_2(^3\Sigma_g^-)$ is reoxidized to give initially Rf radical and $O_2^{\bullet-}$ (process [15]) and finally Rf and H_2O_2 (process [16]). Under these reaction conditions, H_2O_2, together with $O_2^{\bullet-}$ could give rise to $HO^{\bullet}$ (process [18]).

Quenching of ^{1}Rf* by IDs

The fluorescent properties of Rf are well known (6). In air-equilibrated methanolic solution, Rf shows a fluorescence emission band centered at 518 nm. The presence of IDs produced a decrease in the intensity of the steady state emission of ^{1}Rf* but the shape of the emission spectrum did not change. The interaction was quantified through time-resolved methods (SPC technique), by monitoring the fluorescence lifetime of ^{1}Rf* in the presence ($^1\tau$) and in the absence ($^1\tau_o$) of different concentrations of IDs. Through a classical Stern–Volmer treatment (Eq. 1), the rate constants ^1k_q (process [3]) were graphically determined (Fig. 3 and Table 1). The fluorescence decay of Rf in MeOH was monoexponencial with a value $^1\tau_o$ of 5.4 ns, in excellent agreement with previous published data (33,34). The quenching of ^{1}Rf* by IDs was only observed at relatively high IDs concentrations. Hence, process [3] was not significant under the typical experimental conditions employed in this work.

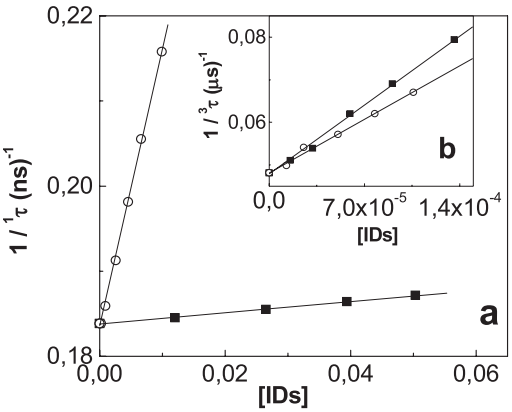

Figure 3. (a) Stern–Volmer plots for the time-resolved quenching of singlet excited riboflavin by (■) tetrahydrozoline and (○) naphazoline. (b) Stern–Volmer plots for the quenching of triplet excited riboflavin by (■) tetrahydrozoline and (○) naphazoline. Solvent: MeOH.

Table 1. Relative rates of oxygen photoconsumption by solutions of NPZ and THZ sensitized by Rf.

	NPZ	THZ
$^1k_q \times 10^{-8}$ (M^{-1}s^{-1})	33.3	1.8
$^3k_q \times 10^{-8}$ (M^{-1}s^{-1})	0.7	3.4
slope$_0$/slope $_{NaN3}$	1.0	1.0
slope$_0$/slope $_{SOD}$	1.0	1.8
slope$_0$/slope $_{CAT}$	1.2	1.7
slope$_0$/slope $_{D\text{-mannitol}}$	1.0	1.7
slope$_0$/slope $_{benzoic\ acid\ sodium\ salt}$	1.0	2.2
Φ_Δ	0.2†	0.08

NPZ = naphazoline; Rf = riboflavin; THZ = tetrahydrozoline; SOD = superoxide dismutase; CAT = catalase.
Rate constants for the quenching of ^{1}Rf* is ^1k_q and ^{3}Rf* is ^3k_q; slope of oxygen uptake sensitized by Rf in the absence (slope$_0$) and in the presence slope$_x$ of different scavengers ($X = NaN_3$, SOD, CAT, D-mannitol or benzoic acid sodium salt) and O_2 ($^1\Delta_g$) quantum yields (Φ_Δ).
†Value taken from Sortino and Scaiano (21).

Laser flash photolysis experiments and the interaction ^{3}Rf*-IDs

^{3}Rf* lifetime, in MeOH, appreciably decreases in the presence of IDs (process [8]), in N_2-saturated solution, demonstrating the occurrence of the interaction between IDs and ^{3}Rf*. As before, a Stern–Volmer treatment of the triplet quenching (Eq. 2) yielded the bimolecular rate constants ^3k_q (Fig. 3, Table 1).

Transient absorption spectrum of Rf, obtained in MeOH 10 μs after the laser pulse (Fig. 4), is similar to the reported one for ^{3}Rf* in MeOH (34). Under identical conditions but in the presence of 5.0 mM NPZ (*ca.* 95% ^{3}Rf* quenched by NPZ), the shape of the long-lived absorption spectrum is in good agreement with that reported for the $RfH^{\bullet}$, a pH 5.1

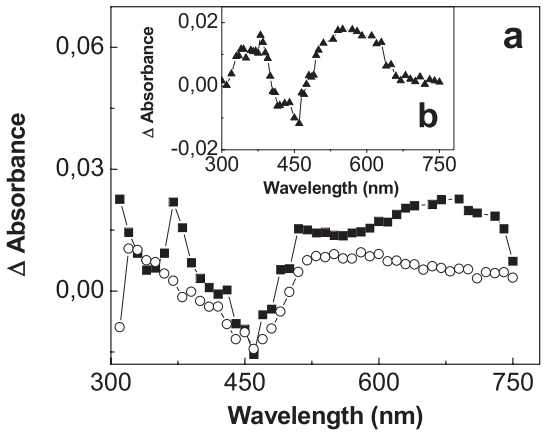

Figure 4. (a) Transient absorption spectra of 0.01 mM riboflavin in N_2-saturated MeOH solution, in the absence (■) and in the presence (○) of 0.5 mM naphazoline. (b) Transient absorption spectra of 0.01 mM riboflavin in N_2-saturated MeOH solution in the presence of 0.1 mM tetrahydrozoline. All taken at 10 μs after the laser pulse.

(26,30,34,35). Besides, the spectrum showed three new peaks centered at 345, 370 and 385 nm, in MeOH. In the presence of THZ (1.0 mM), the shape of the transient absorption spectrum in the absorption region of Rf is similar to that in the case of NPZ (Fig. 4). The time evolution of the ratio of the absorbance at 345 and 380 nm, in the presence of IDs (data not shown), suggests that after almost total decay of the 385 nm band, the 345 nm band becomes better defined, revealing the presence of longer-lived absorbing species mainly at this wavelength. The result for NPZ is in concordance with that previously reported by Sortino and Scaiano (21) in a N_2-saturated NPZ methanolic solution, upon direct photoirradiation with a 308 nm laser excitation, and attributed to the radical species $NPZ^{\bullet+}$.

Participation of reactive oxygen species

To establish the possible involvement of ROS in the evolution of the photoirradiated mixtures, experiments of oxygen uptake upon Rf-photosensitized irradiation were made, in the absence and in the presence of different additives with ROS-scavenging capacity: NaN_3, SOD, CAT and D-mannitol. The quenchers have been already employed in similar concentrations to those utilized in the present work, to confirm/discard the participation of $O_2(^1\Delta_g)$, $O_2^{\bullet-}$, H_2O_2 and $HO^{\bullet}$, respectively, in a given oxidative event (10,23,36–43). NaN_3 physically quenches $O_2(^1\Delta_g)$ (reaction [10]) with a rate constant $k_q = 3 \times 10^8$ M^{-1} s^{-1} in water (23). The enzyme SOD dismutates the species $O_2^{\bullet-}$, through reaction [23] whereas CAT decomposes H_2O_2 as shown (10) in reaction [24] and D-mannitol reacts with the species $HO^{\bullet}$ with a second-order rate constant of 1.9×10^9 M^{-1} s^{-1} in water (38) (reaction [25]).

$$2O_2^{\bullet-} + 2H^+ + SOD \rightarrow O_2(^3\textstyle\sum_g^-) + H_2O_2 \qquad [23]$$

$$2H_2O_2 + CAT \rightarrow 2H_2O + O_2(^3\textstyle\sum_g^-) \qquad [24]$$

$$HO^{\bullet} + D-mannitol \rightarrow products \qquad [25]$$

The rate of oxygen consumption of the individual IDs/Rf system was practically the same in the presence of 5.0 mM NaN_3. Furthermore, when air-equilibrated aqueous solutions of 5.0 mM IDs were photolysed with visible light in the presence of 0.08 mM PN, a recognized O_2 ($^1\Delta_g$) generator (44), no spectral modifications in the UV–visible region were observed. In addition, no oxygen consumption could be detected when aqueous solutions containing IDs (5.0 mM) and 0.08 mM PN were photolysed, even after relatively prolonged irradiation times. In parallel, time-resolved O_2 ($^1\Delta_g$) phosphorescence was evaluated in the presence and in the absence of IDs by means of the TRPD technique. The presence of individual IDs, up to concentrations *ca.* 10 mM, did not affect the O_2 ($^1\Delta_g$) lifetime. An upper limit of 3×10^{-5} M^{-1}s^{-1} for the rate constant k_t was quoted ($k_t = k_q + k_r$, processes [10] and [11], respectively, in Scheme 2). This estimation was made assuming the neat evaluation of ±3% in the O_2 ($^1\Delta_g$) lifetime value, in the range 20–80 μs. Other imidazolines such as xylometazoline, with a chemical structure similar to NPZ and THZ, does not quench O_2 ($^1\Delta_g$). Oxymetazoline, an imidazoline possessing a phenolic group, quenches singlet oxygen with $k_t \sim 10^8$ M^{-1}s^{-1} (S. Criado and N. A. García, 2008, unpublished results). It is well known that phenol group, *per se* is a moderate O_2 ($^1\Delta_g$) quencher (45). Clearly, this additional experimental evidence confirms the absence of noticeable interaction of IDs with O_2 ($^1\Delta_g$).

In the comparative aerobic irradiations, the rate of oxygen uptake was the same for the system 0.02 mM Rf + 5.0 mM NPZ in the absence and in the presence of either 1 mg per 100 mL SOD or 5.0 mM D-mannitol (or 5.0 mM benzoic acid sodium salt). Nevertheless, the addition of CAT (1 mg per 100 mL) to the system 0.02 mM Rf + 5.0 mM NPZ produced a decrease in the rate of oxygen consumption when exposed to light (Fig. 5). When the same system was photolysed in the absence of CAT—and the enzyme added only after ending the photoirradiation—a recovery of the O_2 level was observed (Fig. 5). We independently tested the reaction between 2.0 mM NPZ and 20.0 mM H_2O_2, in aqueous solution. A decrease in the NPZ fluorescence intensity upon addition of the peroxide indicates the occurrence of chemical transformations in the imidazoline.

For the system 0.02 mM Rf + 5.0 mM THZ (Fig. 6), the rate of oxygen consumption was neatly reduced in the comparative aerobic irradiations in the presence of: (1) 1 mg per 100 mL CAT; (2) 1 mg per 100 mL SOD, (3) 5.0 mM D-mannitol and (4) 5.0 mM benzoic acid sodium salt (40).

As additional information, and to eliminate possible interference of the quenchers in the oxygen uptake experiments, SOD, benzoic acid sodium salt and D-mannitol were checked to control that they neither produced a noticeable oxygen uptake when exposed to light in the presence of 0.02 mM Rf, nor interacted with any electronically excited state of the vitamin, under the experimental conditions employed in this work. The last asseveration is also valid for CAT, whereas the enzyme, in the described conditions, produced a negligible oxygen consumption, estimated as *ca.* 10% when compared with the corresponding values for IDs.

The values of the relative rates of oxygen uptake in the presence and in the absence of specific quenchers of ROS are shown in Table 1. These rates constitute the mean values of

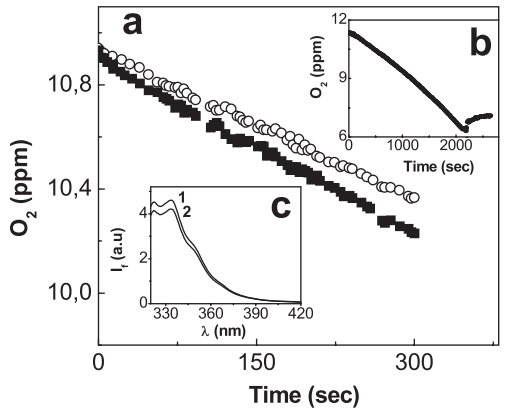

Figure 5. (a) Profiles of oxygen consumption as a function of irradiation time (irradiation wavelength higher than 300 nm): (■) 0.02 mM riboflavin + 5.0 mM naphazoline; (○) 0.02 mM riboflavin + 5.0 mM naphazoline + 1 mg per 100 mL catalase. (b) 0.02 mM riboflavin + 5.0 mM naphazoline + 1 mg per 100 mL catalase, but in this case catalase was added in the absence of light and after an irradiation time of 2100 s. (c) Fluorescence spectra: 1, 2.0 mM naphazoline and 2, 2.0 mM naphazoline + 20.0 mM H_2O_2.

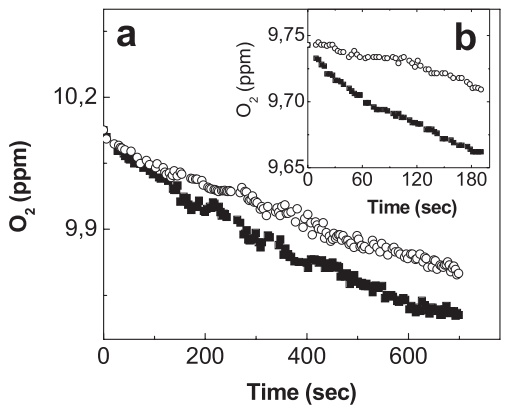

Figure 6. (a) Oxygen consumption upon 0.02 mM riboflavin-sensitized photoirradiation at wavelength higher than 300 nm: (■) 0.02 mM riboflavin + 5.0 mM tetrahydrozoline and (○) 0.02 mM riboflavin + 5.0 mM tetrahydrozoline + 1 mg per 100 mL catalase. (b) (■) 0.02 mM riboflavin + 5.0 mM tetrahydrozoline and (○) 0.02 mM riboflavin + 5.0 mM tetrahydrozoline + 1 mg per 100 mL superoxide dismutase. Solvent: H_2O.

three independent runs which do not differ over 3% from each other.

O_2 ($^1\Delta_g$) quantum yields (Φ_Δ) for IDs

It has been reported that NPZ, upon direct 308 nm photoexcitation, generates $O_2(^1\Delta_g)$ with a quantum yield (Φ_Δ) of 0.2 in MeCN (21). A Φ_Δ value of 0.08 for THZ in the same solvent, upon excitation with an Nd:YAG laser at 266 nm, was determined, employing NPZ as a reference.

DISCUSSION

An initial coarse evaluation of the results indicates that the Rf-sensitized aerobic irradiation of IDs produces chemical transformations clearly observable in the range of the spectral IDs absorption. On the other hand, the photoproducts obtained under aerobic and anaerobic conditions of each ID upon Rf-sensitized irradiation are different, indicating that the species O_2 ($^3\Sigma_g^-$) participates, directly or indirectly, in the photo-oxidation mechanism of IDs. Additionally, oxygen uptake experiments show the participation of ROS generated by Rf electronically excited states. From these results, it is possible to extract important information on potential damage of IDs because of exposure to environmental light in the presence of the vitamin. The identification of the oxygenated reactive species involved in the reaction with IDs, and the extent to which each species participates in the overall photodegradation event are also important.

Although the quenching of ^{1}Rf* was observed in MeOH at relatively high IDs concentration, this process (process [3]) is not significant under the experimental conditions employed in the present work. As a consequence, it can be assumed that the population of ^{3}Rf* is practically not affected by any quenching effect of ^{1}Rf*, employing IDs in the millimolar concentration range.

Regarding the oxygen consumption observed upon Rf-sensitized irradiation of IDs, the reported quantum yield values for the generation by ^{3}Rf* of $O_2(^1\Delta_g)$ (process [7]) and of $O_2^{\bullet-}$ (process not shown in Scheme 2) are 0.5 and 0.009, respectively (46). Hence, in comparative terms, the direct generation of $O_2^{\bullet-}$ by electron transfer from ^{3}Rf* to dissolved oxygen must be considered negligible.

On the other hand, the unambiguous experimental evidence of TRPD results, the absence of oxygen consumption, the spectral modifications upon PN-sensitized photoirradiation of IDs and the lack of any effect exerted by NaN_3 banish a significant participation of a $O_2(^1\Delta_g)$-mediated mechanism. This result is in agreement with previous results by Sortino and Scaiano (21).

It is currently accepted (47) that the quenching of ^{3}Rf* by O_2 ($^3\Sigma_g^-$), to produce $O_2(^1\Delta_g)$ (process [7]) occurs with a rate constant $k_{ET} \approx 1/9$ diffusional value $\approx 1.2 \times 10^9$ M^{-1}s^{-1}, in MeOH. Considering the respective values for ^3k_q (process [8]) in the same solvent (Table 1) for the concentrations of IDs employed in the stationary photolysis experiments (5 mM) and the oxygen concentration in an air-saturated MeOH solution (2.0 mM) (48), it arises that $O_2(^1\Delta_g)$ (process [7]) is formed *ca.* 7 and 1.5 times faster than $Rf^{\bullet-}$ (process [8]) for NPZ and THZ, respectively. In other words, processes [7] and [8] for the cases of both IDs are competitive.

Results indicate that the quenching of ^{3}Rf* by IDs in MeOH is because of an electron transfer process towards Rf, with the concomitant production of $Rf^{\bullet-}$ and $IDs^{\bullet+}$ (process [8] in Scheme 2). We observe that the shape of the transient absorption spectra of Rf in the presence of NPZ or THZ shows the simultaneous presence of the species $RfH^\bullet$ and $IDs^{\bullet+}$. Upto 450 nm the spectral shape is similar to the spectra published (30) for $RfH^\bullet$ a pH 5.1, indicating that in MeOH, effectively, this species is formed. Furthermore, the spectral shape in the region of 300–400 nm is quite similar for both IDs (Fig. 4) and should be attributed to the species $NPZ^{\bullet+}$ and $THZ^{\bullet+}$. Similar peaks in that spectral region have been assigned to $NPZ^{\bullet+}$, in aqueous solution, by Sortino and Scaiano (21). These authors confirmed this result through the oxidation of NPZ with the $SO_4^{\bullet-}$ formed from photolysis of $K_2S_sO_8$ at 266 nm (21).

Neutral Rf radical has been detected as a product of electron transfer processes to $^3Rf^*$ from different electron-donor substrates of environmental and biological relevance (6,49,50). This species triggers a cascade of photoprocesses that may produce the oxidative species $O_2^{\bullet-}$, H_2O_2 and/or $HO^\bullet$ (Scheme 2) that in a further step can react with IDs or with the very sensitizer. The species $RfH^\bullet$ may be formed in the presence of proton donating species (30) (process [13]). It is known (30) that the production of $O_2^{\bullet-}$ by $RfH^\bullet$ occurs with a lower rate than by reaction [20]. The bimolecular decay of $RfH^\bullet$ can yield Rf and RfH_2 (process [14]), which, in the presence of O_2 ($^3\Sigma_g$) can be reoxidized, regenerating Rf and producing H_2O_2 (process [15–16]). Under these conditions, H_2O_2, together with $O_2^{\bullet-}$ can give rise to $HO^\bullet$ through an Haber–Weiss reaction (process [18]) and, in consequence, three ROS, besides the already discussed O_2 ($^1\Delta_g$), can be present in the medium. The recovery of the vitamin, through processes [14], [16] and [20], represents a crucial step in living organisms, for which it is well established that ROS are a key intermediate in the oxygen redox chemistry (29).

The neat delay observed in the rate of oxygen uptake during the Rf-sensitized irradiation of NPZ in the presence of CAT, strongly suggests the participation of H_2O_2 in the oxidative process. The generation of H_2O_2 as a consequence of the exposure to light was also demonstrated when CAT was added to the system Rf + NPZ after irradiation, and an increase of the $O_2(^3\Sigma_g^-)$ was observed. This enzyme transforms the H_2O_2 produced into H_2O and O_2, compensating the uptake of O_2 (reaction [24]). The result obtained from the direct reaction between NPZ and H_2O_2 strongly supports the participation of this ROS in the Rf-sensitized oxidation of NPZ. In parallel, the lack of any effect on the oxygen consumption in the presence of SOD and D-mannitol (or benzoic acid sodium salt) leads us to discard a noticeable participation of $O_2^{\bullet-}$ and $HO^\bullet$ as oxidative agents. The generation of H_2O_2 as a consequence of light-exposure was also demonstrated when CAT was added to the system Rf-NPZ after photoirradiation. An increase of the overall oxygen content was observed (Fig. 5) as a result of reaction [24].

The case of THZ is somewhat different. The decrease in the rate of oxygen consumption in the photoirradiated system Rf-THZ in the presence of SOD, CAT and D-mannitol (or benzoic acid sodium salt), accounting for the respective presence of $O_2^{\bullet-}$, H_2O_2 and $HO^\bullet$, suggests that the oxidative mechanism is not simple, although all three oxidative species may be generated and may potentially react with THZ. $RfH^\bullet$ and $O_2^{\bullet-}$ are straightforwardly generated from $Rf^{\bullet-}$ (processes [13] and [20], respectively) and act, according to Scheme 2, as precursors of the species H_2O_2 and $HO^\bullet$ (processes [15–16] and [18]). Hence, a decrease in the rate of oxygen uptake with SOD present may be accounting for a process $O_2^{\bullet-}$-mediated exclusively (processes [20–21]) but also an H_2O_2- or an $HO^\bullet$-mediated oxidation, because the generation of these species needs the presence of $O_2^{\bullet-}$. Similarly, the generation of $HO^\bullet$ depends on the previous H_2O_2 and $O_2^{\bullet-}$ generation (reaction [18]). Again, the scavenging of either of the two species will reduce the rate of oxygen uptake in a $HO^\bullet$-mediated THZ oxidation. Following this line of reasoning, $HO^\bullet$ is the only species that may be independently detected. As said, the SOD test effectively recognizes the presence of $O_2^{\bullet-}$ as an initial oxidative species, but does not demonstrate the direct participation of this ROS in the oxidative process. $HO^\bullet$ is a final species and may be intercepted by D-mannitol and benzoic acid sodium salt. Although other radicals such as alkyl-peroxy could also react with $HO^\bullet$, their presence in our system is not evident. Hence, on the basis of the available experimental evidence, the interaction of THZ with $HO^\bullet$ remains a possibility.

The relative long lifetime of $^3NPZ^*$ (*ca.* 15 μs, in aqueous solution pH 7.4) and the value of the quenching rate constant observed in the presence of O_2 ($^3\Sigma_g^-$) (1.8×10^9 $M^{-1}s^{-1}$), in aqueous solution pH 7.4) suggest that $^3NPZ^*$ could sensitize $O_2(^1\Delta_g)$ formation through energy transfer to O_2 ($^3\Sigma_g^-$), in the millimolar concentration range (21,51,52). The generation of O_2 ($^1\Delta_g$) from the lowest excited state of THZ, upon direct UV light irradiation, was observed. Φ_Δ value is in the reported range (21) for NPZ (0.2 ± 0.02 at $\lambda = 308$ nm, in MeCN). Regarding the Φ_Δ values, NPZ and THZ appear as relatively good O_2 ($^1\Delta_g$) sensitizers. In spite of the fact that self-promoted oxidation of IDs *via* O_2 ($^1\Delta_g$) could be discarded, the sensitized oxidation of surrounding molecules can occur.

From the results obtained under aerobic and anaerobic conditions, we postulate that the Rf-sensitized photo-oxidation of NPZ and THZ proceeds *via* two mechanisms and the ROS involved in both are different too. Nevertheless, the radical cation formed ($IDs^{\bullet+}$) from $^3Rf^*$ is identical for both IDs.

In spite of the fact that NPZ seems to be more resistant to photogenerated ROS, in comparison to THZ, the former can be considered a fairly good photodynamic sensitizer, therefore the sensitized degradation of different molecules present in a biological media could be produced.

Acknowledgements—Financial support from Consejo Nacional de Investigaciones Científicas y Técnicas (CONICET), Agencia Nacional de Promoción Científica y Tecnológica (ANPCyT) and Secretaría de Ciencia y Técnica de la Universidad Nacional de Río Cuarto (SECyT UNRC), all from Argentina, is gratefully acknowledged.

REFERENCES

1. Straight, R. C. and J. D. Spikes (1985) Photosensitized oxidation of biomolecules. In *Singlet Oxygen*, Vol. 4 (Edited by A. A. Frimer), pp. 91–143. CRC Press, Inc., Boca Raton.
2. Albini, A. and E. Fasani (1998) *Drugs. Photochemistry and Photostability*. The Royal Society of Chemistry, Cambridge.
3. Sortino, S., G. Cosa and J. C. Scaiano (2000) pH effect on the efficiency of the photodeactivation pathways of naphazoline: A combined steady state and time resolved study. *New J. Chem.* **24**, 159–163.
4. Roberts, J. E. (1996) Ocular phototoxicity. In *Dermatotoxicology*, Chap. 24 (Edited by F. Marzulli and M. Maiback), pp. 307–313. Taylor and Francis, Washington, DC.
5. Roberts, J. E. (2001) Ocular phototoxicity. *J. Photochem. Photobiol. B: Biol.* **64**, 136–143.
6. Heelis, P. F. (1982) The photophysical and photochemical properties of flavins (isoalloxazines). *Chem. Soc. Rev.* **11**, 15–39.
7. Wollensak, G., E. Spoerl and T. Seiler (2003) Riboflavin/ultraviolet-A-induced collagen crosslinking for the treatment of keratoconus. *Am. J. Ophthalmol.* **135**, 5, 620–627.
8. Spoerl, E., G. Wollensak, D.-D. Dittert and T. Seiler (2004) Thermomechanical behavior of collagen-cross-linked porcine cornea. *Ophthalmologica* **218**, 136–140.
9. Wollensak, G. (2006) Crosslinking treatment of progressive keratoconus: New hope. *Curr. Opin. Ophthalmol.* **17**, 4, 356–360.
10. Silva, E., R. Ugarte, A. Andrade and A. M. Edwards (1994) Riboflavin-sensitised photoprocesses of tryptophan. *J. Photochem. Photobiol. B: Biol.* **23**, 43–48.

11. Silva, E., V. Ruckert, E. Lissi and E. Abuin (1991) Effects of pH and ionic micelles on the riboflavin-sensitized photoprocesses of tryptophan. *J. Photochem. Photobiol. B: Biol.* **11**, 57–68.
12. Zimniak, P. (2008) Detoxification reactions: Relevance to aging. *Ageing Res. Rev.* **7**, 281–300.
13. Godley, B. F., F. A. Shamsi, F. Q. Liang, S. G. Jarret, S. Davies and M. E. Boulton (2005) Blue light induces mitochondrial DNA damage and free radical production in epithelial cells. *J. Biol. Chem.* **280**, 21061–21066.
14. Kanofsky, J. R., P. D. Sima and C. Richter (2003) Singlet-oxygen generation from A2E. *Photochem. Photobiol.* **77**, 235–242.
15. Rosanowska, M., J. Jarvis-Evans, W. Korytowski, M. E. Boulton, J. M. Burke and T. Sarna (1995) Blue light-reactivity of retinal pigment. In vitro generation of oxygen-reactive species. *J. Biol. Chem.* **270**, 18825–18830.
16. Lev, R. and R. Clark (1995) Visine® overdose: Case report of an adult with hemodynamic compromise. *J. Emerg. Med.* **13**, 649–652.
17. Potter, D. E. and M. J. Ogidigben (1991) Meditomidine-induced alterations of intraocular pressure and contraction of the nictitating membrane. *Invest. Ophthalmol. Vis. Sci.* **32**, 2799–2805.
18. Bousquet, P., J. Feidman, E. Tibrica, G. Bricca, A. Molines, M. Dontenwill and A. Belcourt (1989) New concepts on the central regulation of blood pressure. Alpha 2-adrenoceptors and ''imidazoline receptors.'' *Am. J. Med.* **87**, 108–138.
19. Chan, C. K. S., F. Sannajust and G. A. Head (1996) Role of imidazolie receptors in the cardiovascular actions of moxonidine, rilmenidine and clonidine in conscious rabbits. *J. Pharmacol. Exp. Ther.* **276**, 411–420.
20. Head, G. A. and F. Sannajust (1992) Importance of imidazolie receptors in the cardiovascular responses of clonidine and rilmenidine in conscious rabbits. *Fundam. Clin. Pharmacol.* **6** (Suppl. 1), S31–S43.
21. Sortino, S. and J. C. Scaiano (1999) Photogeneration of hydrated electrons, nitrogen-centered radicals and singlet oxygen from naphazoline: A laser flash photolysis study. *Photochem. Photobiol.* **70**, 590–595.
22. Criado, S., S. G. Bertolotti and N. A. García (1996) Kinetic aspects of the rose bengal sensitised photooxygenation of tryptophan alkyl esters. Ground state and photopromoted dye-tryptophan derivative interactions. *J. Photochem. Photobiol. B: Biol.* **34**, 79–86.
23. Wilkinson, F., W. Helman and A. B. Ross (1995) Rate constants for the decay of the lowest electronically excited singlet state molecular oxygen in solution. An expanded and revised compilation. *J. Phys. Chem. Ref. Data* **24**, 663–1021.
24. Foote, C. S. and T.-Y. Ching (1975) Chemistry of singlet oxygen XXI. Kinetics of bilirubin photooxygenation. *J. Am. Chem. Soc.* **97**, 6209–6214.
25. Slifkin, M. (1971) *Charge Transfer Interactions of Biomolecules*. Academic Press, London.
26. Chacón, J. N., J. McLearie and R. S. Sinclair (1988) Singlet oxygen yields and radical contribution in the dye-sensitized photooxidation in MeOH of esters of polyunsatured fatty acids (oleic, linoleic, linolenic and arakidonic). *Photochem. Photobiol.* **47**, 647–656.
27. Heelis, P. F. (1991) The photochemistry of flavins. In *Chemistry and Biochemistry of Flavoenzymes*, Vol. 1 (Edited by F. Muller), pp. 171–193. CRC Press, Inc., Boca Raton.
28. Lu, C., G. Bucher and W. Sander (2004) Photoinduced interaction between oxidized and reduced lipoic acid and riboflavin (Vitamin B2). *Phys. Chem. Phys.* **5**, 47–56.
29. Kanofsky, J. R. (1991) Singlet oxygen production from the reaction of superoxide ion an aprotic solvents: Implications for hydrophobic biochemistry. *Free Radic. Res. Commun.* **87**, 12–13.
30. Land, E. J. and A. J. Swallow (1969) One-electron reactions in biochemical systems as studied by pulse radiolysis. II Riboflavin. *Biochemistry* **8**, 2117–2125.
31. Lu, C. Y., W. Z. Lin, Z. H. Wang, Z. H. Han, S. D. Yao and N. Y. Lin (2000) Riboflavin (VB_2) photosensitised oxidation of 2′-deoxyguanosine-5′-monophosphate (dGMP) in aqueous solution: A transient intermediates study. *Phys. Chem. Phys.* **2**, 329–334.
32. Lu, C. Y., W. F. Wang, W. Z. Lin, Z. H. Han, S. D. Yao and N. Y. Lin (1999) Generation and photosensitisation properties of the oxidized radicals of riboflavin: A laser flash photolysis study. *J. Photochem. Photobiol. B: Biol.* **52**, 111–116.
33. Bertolotti, S. G., C. M. Previtali, A. M. Rufs and M. V. Encinas (1999) Riboflavin/triethanolamine as photoinitiator system of vinyl polymerization. A mechanistic study by laser flash photolysis. *Macromolecules* **32**, 2920–2924.
34. Criado, S. and N. A. García (2004) Vitamin B_2-sensitised photooxidation of the ophthalmic drugs Timolol and pindolol. Kinetics and mechanism. *Red. Rep.* **9**, 291–297.
35. El Hanine-Lmoumene, C. and L. Lindqvist (1997) Stepwise two-photon excitation of 1,5-dihydroflavin mononucleotide: Study of flavosemiquinone properties. *Photochem. Photobiol.* **66**, 591–597.
36. Baxter, R. M. and J. H. Carey (1983) Evidence for photochemical generation of superoxide ion in humic waters. *Nature* **306**, 575–576.
37. Zang, L.-Y. and H. P. Misra (1992) Superoxide radical production during the autoxidation of 1-methyl-4-phenyl-2,3-dihydroxypyridinium perchlorate. *J. Biol. Chem.* **267**, 17547–17552.
38. Iuliano, L., D. Pratico, A. Ghiselli, M. S. Bonavita and F. Violi (1992) Reaction of dipyridamole with hydroxyl radical. *Lipids* **27**, 349–353.
39. Tratniek, P. G. and J. Hoignè (1991) Oxidation of substituted phenols in the environment: A QSAR analysis of rate constants for reaction with singlet oxygen. *Environ. Sci. Technol.* **25**, 1596–1604.
40. Silva, E., L. Herrera, A. M. Edwards, J. De la Fuente and E. Lissi (2005) Enhancement of riboflavin-mediated photo-oxidation of glucose 6-phosphate dehydrogenase by uronic acid. *Photochem. Photobiol.* **81**, 206–211.
41. Silva, E., A. M. Edwards and D. Pacheco (1999) Visible light-induced photooxidation of glucose sensitised by riboflavin. *J. Nutr. Biochem.* **10**, 181–185.
42. Cohen, G. and R. E. Heikkila (1974) The generation of hydrogen peroxide, superoxide radical and hydroxyl radical by 6-hydroxydopamine, dialuric acid and related cytotoxic agents. *J. Biol. Chem.* **249**, 2447–2453.
43. Frati, E., A.-M. Khatib, P. Front, A. Panasyuk, F. Aprile and R. D. Mitrovic (1997) Degradation of hyaluronic acid by photosensitised riboflavin *in vitro*. Modulation of the effect by transition metals, radicals quenchers and metal chelators. *Free Radic. Biol. Med.* **22**, 1139–1144.
44. Martí, C., O. Jürgens, O. Cuenca, M. Casals and S. Nonell (1996) Aromatic ketones as standards for singlet molecular oxygen photosensitisation. Time-resolved photoacustic and near-IR emission studies. *J. Photochem. Photobiol. A: Chem.* **97**, 11–18.
45. García, N. A. (1994) Singlet molecular oxygen-mediated photodegradation of aquatic phenolic pollutants. *J. Photochem. Photobiol. B: Biol.* **22**, 185–196.
46. Krishna, C. M., S. Uppuluri, P. Riesz, J. S. Zigler and D. Balasubramanian (1991) A study on the photolysis efficiencies of some lens constituents. *Photochem. Photobiol.* **54**, 51–56.
47. Koizumi, M., S. Kato, N. Mataga, T. Matsura and I. Isui (1978) *Photosensitised Reactions*. Kagakudogin, Kyoto.
48. Murov, S. L. (1973) *Handbook of Photochemistry*, p. 89. M. Decker, New York.
49. Pajares, A., J. Gianotti, G. Stettler, S. Bertolotti, S. Criado, A. Posadaz, F. Amat-Guerri and N. A. García (2001) Modelling the natural photodegradation of water contaminants: A kinetic study on the light-induced interactions between riboflavin and 4-hydroxypyridine. *J. Photochem. Photobiol. A: Chem.* **139**, 199–204.
50. Haggi, E., S. Bertolotti, S. Miskoski, F. Amat-Guerri and N. A. García (2002) Environmental photodegradation of pyrimidine fungicides. Kinetics of the visible-light-promoted interactions between riboflavin and 2-amino-4-hydroxy-6-methylpyrimidine. *Can. J. Chem.* **80**, 62–67.
51. Sortino, S., S. Giuffrida and J. C. Scaiano (1999) Phototoxicity of naphazoline. Evidence that hydrated electrons, nitrogen-centered radicals and OH radicals trigger DNA damage: A combined photocleavage and laser flash photolysis study. *Chem. Res. Toxicol.* **12**, 971–978.
52. Bensasson, R. V., E. J. Land and T. G. Truscott (1983) *Flash Photolysis and Pulse Radiolysis*, Chap. 4. Pergamon Press, Oxford.